THE UNIVERSITY OF QUEENSLAND

Fire Performance of High Strength Concrete using a Novel Fire Testing Method

Student Name: Yanfeng ZHU

Course Code: ENGG7240

Supervisor: Dr Vinh Dao

Submission date: 27 October 2017

Faculty of Engineering, Architecture and Information Technology

Abstract

Due to the degradation of high strength concrete performance(HSC) at elevated temperature, it is of great significance to have a detailed knowledge of the properties of HSC at elevated temperature. In conventional fire tests, furnaces are commonly employed to heat concrete. However, the thermal boundary condition provided by furnaces has been proven inconsistent and unreliable. The results achieved through conventional fire tests should be re-examined. In order to solve this problem, a novel fire testing method using radiant panel system is introduced. It is able to set up a consistent, reliable and uniform thermal boundary condition in fire resistance test of HSC. Furthermore, two digital information capturing methods: Digital Image Correlation(DIC) and actuator are applied to measure the deformation of HSC during the test. A series of solutions are proposed to deal with the limitations of these two methods and reliable measurement is achieved. Moreover, the fire performance of HSC is examined using this novel testing method under three conditions: ambient temperature test, unstressed-hot test and stress-hot test. The results demonstrate the compression strength, stress-strain curve and elastic modulus of HSC at ambient temperature and elevated temperature.

Contents

List of figures

Chapter 1. Introduction

1.1 Background

In recent days, high strength concrete(HSC) has an increasing trend of application in high buildings, bridges and dams due to its favorable properties. One of them is fire resistance, including high specific heat, non-combustibility, low thermal conductivity and non-emission of smoke or toxic gases. However, when HSC is exposed to elevated temperature, it has a faster degradation of mechanical property than normal strength concrete(NSC) and is more likely to be explosively spalled(Chan, Peng, & Chan, 1996). Therefore, in order to guarantee the safety of constructions in fire, it is of great importance to examine the performance of HSC in high temperature. In this paper, HSC refers to the concrete of which the compressive strength is not less than 60 MPa(Cement, amp, & Aggregates, 2010).

Although a large number of studies in this area have already been done over the past decades, most findings of mechanical properties of concrete in high temperature are based on the conventional fire tests, in which conventional funaces or ovens are applied(Castillo, 1987; Ingberg, Griffin, Robinson, & Wilson, 1921; Khoury, Grainger, & Sullivan, 1985). However, it has been stated that the data colllected in this method are not realiable as conventional funaces or ovens are not able to provide a consistent thermal boundary condition to concrete (Torero, 2014). Thus, a reliable , well-controlled and repeatable thermal boundary condition is required in the fire resistance test of HSC.

Another ciritial part in fire tests of conrete is the deformation measurement method, which can be divided into contanct method and non-contact method. Each type of the method has its own limitations. For example, high-temperature strain gauges as one contact measurement method have poor performance in terms of thermal response when they exposed to evevated temperature (McAllister et al., 2012). And laser sensors as a non-contact method have high cost, leading to the restricted application in concrete tests. Therefore, proper solutions to these challenges are required to get a reliable deformation measurement.

1.2 Objectives of thesis

In this paper, instead of standard furnaces or ovens, a novel fire testing method is applied to figure out the fire performance of HSC when exposed to elevated temperature. The key ojectives of this thesis can be summarized as follows:

i. Set up reliable thermal boundary conditions which can be applied into the fire

resistance test of HSC;

ii. Apply two different deformation measurement methods in the experoment to achieve a realiable deformantion measurement;

iii. Examine mechanical properties of HSC in high temperature through data collecting and numerical analysis. After this, a comparision will be made between the properties of HSC in high temperature and in ambient temperature, including compressive strength and elastic modulus.

1.3 Scope of thesis

This thesis is limited to HSC which follows Australian Standards (AS 1012.8.1, 2014). After casting for 24 hours and being demolded, all the specimens were placed in water tanks for six days and then kept in a curing room with 23℃ and 50% relative humidity. The specimens are HSC cylinders 200 mm high by 100 mm diameter with f'c = 80 MPa. In the fire resistance tests, the level of incident heat flux is 20kW/m^2, and the pre-compressive stress is selected as 20% of ultimate strength at ambient temperature (around 25 ℃). The target temperatures during the tests include ambient (around 25 ℃) and 150 ℃.

1.4 Outline

This thesis report has five chapters. After an introduction of the thesis in Chapter 1, a literature review is made in Chapter 2. It firstly reviews the conventional fore tests of concrete using a funace and points out the limitaitons in the tests. Then deformantion mearsurement methods including contact and non-contact menthos are introduced as well as the challenges of them. After this, it focuses on the themal properties and mechanical properties of concrete at elevated temperature. In Chapter 3, the detalis of the experiments are illustrated, including how to set up a consistent and repeatable thermal boundary condition, as well as how to apply actuator and DIC the measure the deformation of HSC cylinders in the tests. The results of the tests are presented in Chapter 4. The compression strength, stress-strain curves and elastic modulus of HSC are achieved under different test conditions. Finally, the conclusions of the whole thesis are made in Chapter 5, and some suggestions for further works are presented.

Chapter 2. Literature Review

This chapter will firstly have a brief introduction of conventional fire tests of concrete and their limitations. Then, it will turn to deformation measurement methods, including contact method and non-contact method. Finally, the properties of concrete in high temperature tested through the prior studies will be reviewed.

2.1 Conventional fire tests of concrete

In 1870, the concept of 'Fire-Proof Construction' was generated after the destruction of several buildings due to fire (Jacob, 1870). After this, the concept was developed due to the increasing concerns on fire safety of concrete constructions. In 1912, a test named "fire and water" became popular among manufactures to examine the material's abiliy of fire resistance(Kendall, 1912; Maluk Zedan, 2014). However, this method was proven to be unrealiable later.

At the beginning of 20th century, experts in America and Europe made a great contribution to unifying fire tests standards (Miller & Stewart, 1902; Sachs, 1903; NFPA, 1914). Sachs (1903) suggested that a fire resistance test should keep a continuous minimum temperature over a characterized timeframe. During this period, conventional furnaces and ovens began to be applied in fire resistance tests of concrete (Fig. 2-1). Figure 2-2 presents the current column test facility whose height is 4300 mm and floor area is 2600*2600 mm2(Mostafaei, 2013). There is a highly similarity between the 1919's furnace and 2013's furnace.

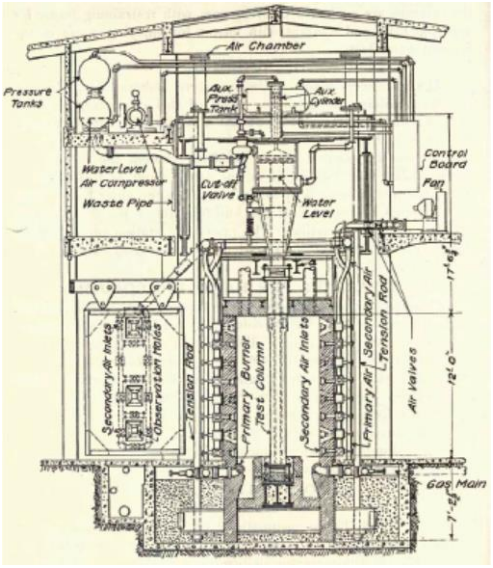

Figure 2-1. An early version of a furnace used in column tests in 1919(C Maluk, 2014).

Figure 2-2. The column test facility (Mostafaei, 2013).

To eaxmaine the fire performance of a structure element, fire resistance period is an imprtant index(Fsh, 2008). It means the time that the material can be exposed to heat in a furnace without failure like structural adequacy and integrity. During heating, the temperature of the funace should be controlled following a temperature-time curve. This is because the gradience of the temperature can directly effect the incident heat flux exposed on the specimen, thereby influcing the heat flux absorbed by the specimen. Equation 2-1 illustrates the relationships among them:

$$q_{abs}'' = \varepsilon (q_{inc}'' - \sigma T_s^4) + h_c \ (T_g - T_s) \qquad \textit{Equation 2-1}$$

where q_{abs}'' is the absorbed heat flux on the surface of specimen; ε refers to the emissivity of a material; q_{inc}'' is the incident heat flux; T_s means the temperature of material's surface; T_g is the temperature of gas and h_c is the convective coefficient .

The temperature-time curve was firstly adopted in a conference in 1918 (Fig. 2-3), and remained almost the same nowadays(Fig. 2-4). In a conventional material fire resistance test using furnaces, the main process are as follows (Le, 2016):

i. Place a specimen into a furnace;

ii. Increase the temperature of furnace at a much slower heating rate than real fire;

iii. Keep heating until the temperature of the specimen has reached the target temperature;

iv. Take the specimen out of the furnace and test it.

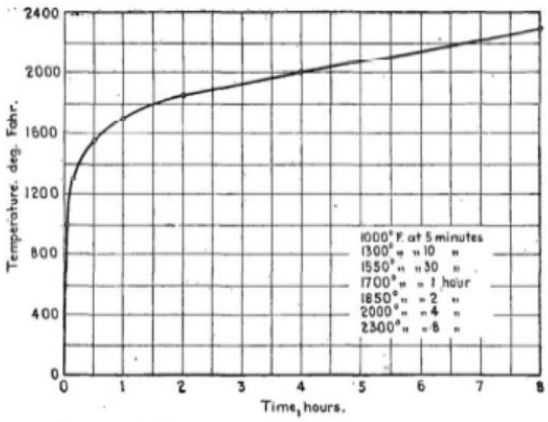

Figure 2-3. Standard time-temperature curve in 1918 (NFPA, 1918).

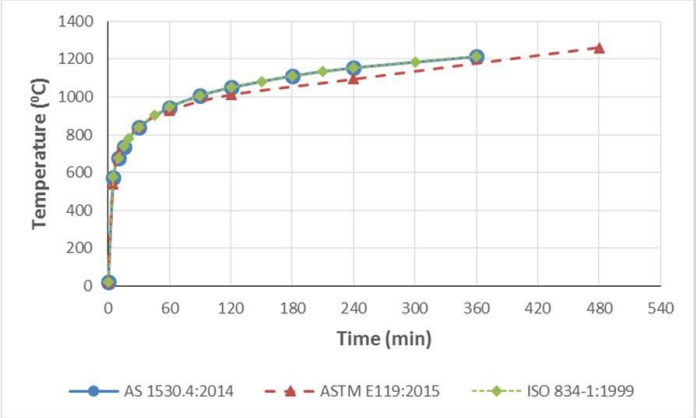

Figure 2-4. Standard Time-Temperature curves in ISO, Australia and America (ISO 834-1, 1999; AS 1530.4:2014, 2014; ASTM E 119, 2015).

However, many studies has proven that the themal boundary condition of the specimens in the funace is lack of realiablity. First, in the furnaces, the incident heat flux is normally provieded by both gas and funaces walls in terms of convection and raiation (Yabuki, Harada& Terai, 1995). As a consequence, the thermal boundary condition can be influenced by the type of the funace and the therml property of funace walls (Torero, 2014). What is more, the average temperature of the furnace during the test is measured by several Type K chromel–alumel thermocouples which are placed in specimen(Mostafaei, 2013). However, it has been stated that there exists a significant difference between furnace temperatures measured by different types of thermocouples, expecially at the begning of the operation(Sultan, 2010). Besides, due to the high costs of furnaces, many specimens were tested in a single furnace at the same time(Anagnostopoulos, Sideris, & Georgiadis, 2009). The interacition of the specimens can lead to negative impacts on the thermal boundary condition of each specimen. Therefore, the conventional funaces are not able to supply a consistent or repeatable thermal boundary condition. In addition, as furnaces are close configuration, they increase the difficiulty to

measure the deformation of specimen during heating.

Due to the disadvantages of funaces in fire resistance test, the results from the prior studies should be re-examined with a more optimum testing method. In 2012, Cristian Maluk et al. introduced a novel fire testing methodology named Heat-Transfer Rate Inducing System (H-TRIS), in which raidant panels were used as the only heat provider (Fig. 2-5). Based on the radiaiton mechanism, H-TRIS can well eliminate the disadvantages of funaces. Therefore, in this project, radiant panels will be applied to offer a consistent and repeatable thermal boundary condition, so that the proformance of HSC in elevated temperature can be well examined.

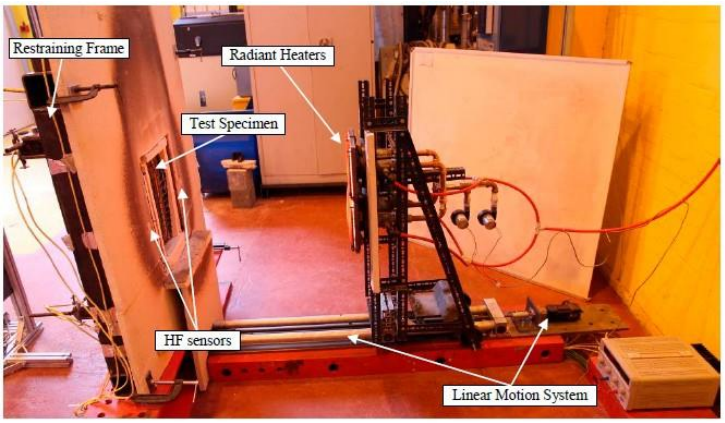

Figure 2-5. Heat-Transfer Rate Inducing System (H-TRIS) (Cristian Maluk et al., 2012).

2.2 Deformation measurement

In fire resistance tests of HSC cyliners, the displacement of the cylinders is required to be detected during heating. The current measurement methods can be mainly classfied into two types: direct-contact method and non-contact method. A brief introudcution of each type and their corresponding limitaitons will be made in the following content.

2.2.1 Contact measurement method

In contact measurement, there are four major methods: actuator, compressometer, strain gauges and linear variable differential transformers (LVDT). One common limitation of these methods is that they can only measure local displacement at some local locations, resulting into a possibility that some important deformation points are missed.

In 1987, Castillo used an actuator equipped with an electric heating furnace (Fig. 2-6) to study the impact of transient high temperature on HSC. The deformation during the test was achieved by the actuator. However, Castillo (1987) pointed out that deformation in the load-deformation curves actually represented the total displacement between the end of the actuator piston and the stationary platen of the testing frame, which means not only the deformation of the specimens, but also the deformation of the testing devices was included. Therefore, the results resulted from actuator are not accurate.

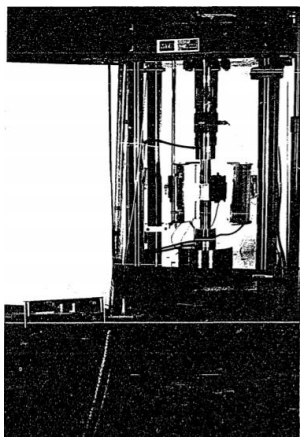

Figure 2-6. Loading frame with the heating furnace(Castillo, 1987).

A compressometer was introduced by the American Society for Testing and Materials (ASTM) in 1961 as a non-destructive method to measure the modulus of elasticity of a concrete cylinder(Voigt, 2010). When the compressometer was connected with a concrete cylinder, the yoke with two screws will rotate as the cylinder was compressed, in which way the defomation of the specimen can be measured. Voigt (2010) stated that compressometer was an suitable method to measure the deformation of concrete at ambient temperature, but had a much lower precision campared with strain gauges and also need more tests to reach a reasonable limit of deviation of the results.

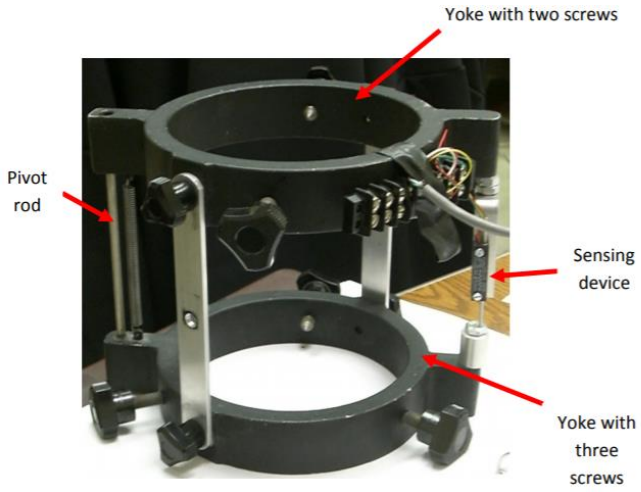

Figure 2-7. Compressometer used in standard C469 Testing(Voigt, 2010).

Another type of compressometer(Fig. 2-8) which can work in high temperature environment was applied to examine the fire performance of HSC (Phan & Carino, 2002). The strain of the specimen was measured by this high-temperature compressometer with a gage length which was placed outside the furnace. Nonetheless, as compressometer can only measure the displacement of specimen before peaking load rather than the whole process, only static elastic modulus of concrete specimen was measured(Phan & Carino, 2002).

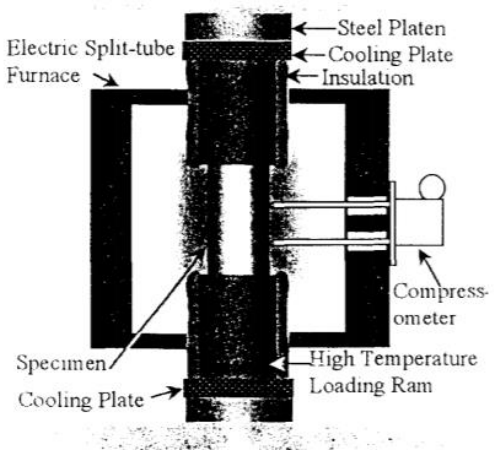

Figure 2-8. Compression machine (Phan & Carino, 2002).

Strain gauges can be attached directly on the surface of specimen and the deformation of the conductor caused by the deformation of the specimen will result in the changes of electrical resistance end-to-end. By measuring the electrical resistance of a strain gauge, the strain can be inferred(Hoffmann, 1989). Nevertheless, when stain gauges are applied in high temperature environment, they become unreliable. Kayser, Godefroy, & Leca (1993) used high-temperature thin-film strain gauges (Fig. 2-9) to plot the stress-strain curve of a material. They stated that there existed a good agreement between theoretical and experimental results at 23℃. However, at high temperature, the difference became significant, which can be resulted from the discrepancy in the gauge factor (K) of the strain gauges. In 2012, McAllister et al. pointed out that the performance of high-temperature strain gauges was poor when exposed to evevated temperature.

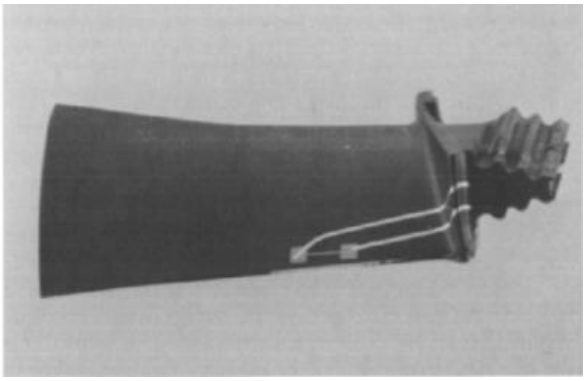

Figure 2-9. A high-temperature strain gauge attached on the specimen(Kayser, Godefroy, & Leca, 1993).

A LVDTs normally contains a fixed coil assembly and a core which is connected to the specimen (Fig. 2-10). The changes of the core will change the voltage in the coil, in which method the deformation of specimen can be measured. LVDTs have been widely used to measure the axial deformationand the results are reliable and long-term stable(Kayser et al.,

1993; Malladi, 2015; Sounthararajah, Wong, Nguyen, Bui, & Kodikara, 2017). Nonetheless, the comlex components and large number of connections in LVDT can generate potential errors in high temperature environment.

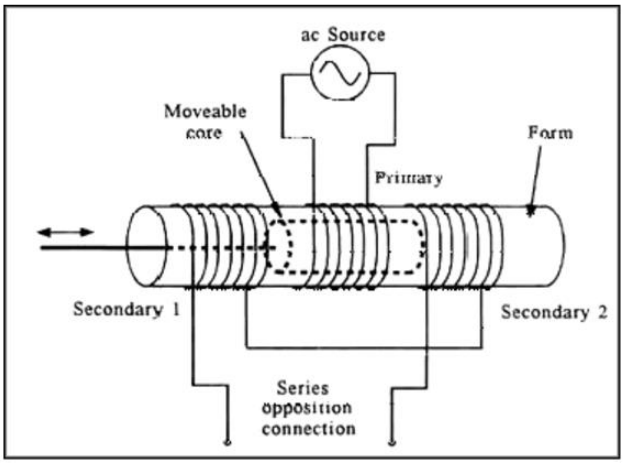

Figure 2-10. General LVDT assembly (Kesavan& Reddy, 2006).

2.2.2 Non-contact measurement method

Non-contact measurement methods mianly include laser displacement sensors(LDS) and Digital Image Correlation (DIC). As this tpye of measurement do not need to have an direct contact with the specimen, the influence caused by the high temperature in the fire resistance tests can be well elimitated.

LDS is mainly made up of scanning platform and control and data acquisition unit (Fig. 2-11). Based on the principle of triangulation measurement, LDS can project laser beam and output the data of the displacement for every measurement point(Giri, Kharkovsky, & Samali, 2017). In ambient temperatures, LDS can detect the deformation with a high level of accuracy. However, when the temperature fluctuates, LDS require 20 minutes to warm up, so that the distribution of temperature in the system can be uniform (Micro-Epsilon, 2008). What is more, the cost of LVD is relatively high, leading to a limited number of applications in fire resistance tests.

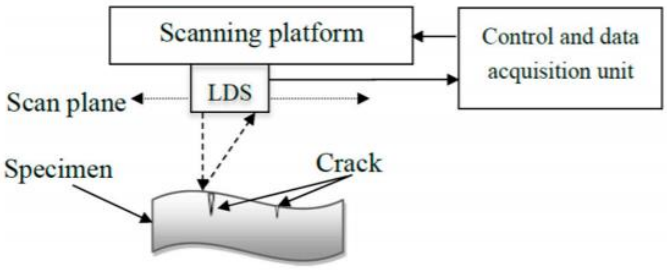

Figure 2-11. Schematic of LDS system (Giri et al., 2017).

DIC is a non-destructive measurement technique to measure the surface deformation of

specime. It will detect the strain by tracking the changes of the speckle patterns on the specimen's surface and computing the changes of length(Yuan, 2014). According to the measurement dimensions of the specimen, DIC can be cllasified into 2D DIC and 3D DIC(Hu, Xie, Lu, Hua, & Zhu, 2010). 2D DIC can only measure the in-plane displacement, while 3D DIC can achieve out-of-plane dosplacement measurement. When DIC is applied into fire resistance tests, one potential difficulty is that the laser beam generated by DIC can be influenced by heat haze or the windows of furnaces. Moreover, in order to achieve a high quality of image, the durability of speckle patterns under high temperature should also be investigated.

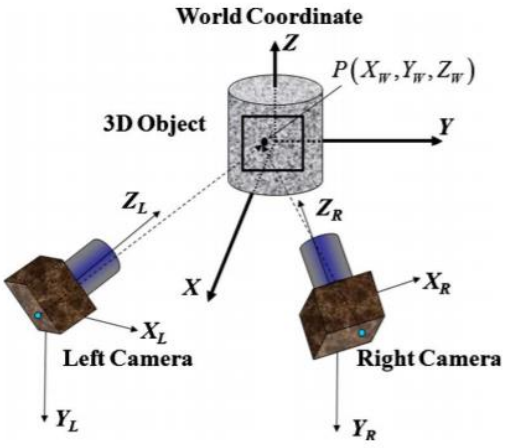

Figure 3-12. Schematic of 3D-DIC system(Hu et al., 2010).

2.3 Properties of concrete

2.3.1. Thermal properties

The thermal properties of HSC when exposed to high temperature mainly include thermal expansion strain, specific heat and thermal conductivity.

a) Thermal expansion strain

Thermal expansion strain can be measured by the displacement gages with are connected with the silica glass on the surface of the specimen (Fig. 2-13). Heating during the tests should be applied at a slow rete and the corresponding temperatures during the test are measured by the thermocouples (Kakae et al., 2017).

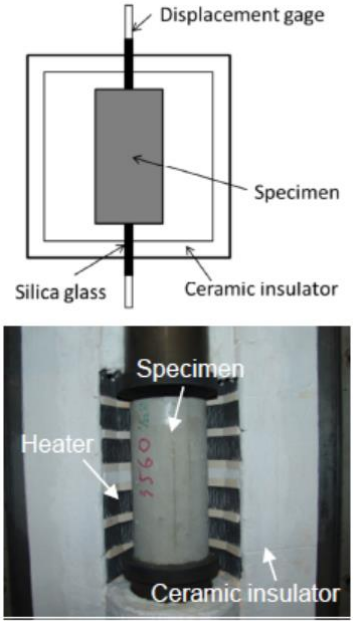

Figure 2-13. Schematic of thermal expansion strain test (Kakae et al., 2017).

b) Specific heat

The specific heat of HSC refers to the amount of heat required to raise the temperature by 1°C of one kilogram of HSC. It can be determined by Equation 2-2:

$$C_p = \frac{W \times \Delta t}{M \times \Delta \theta} - \frac{M' \times C'}{M} \qquad \textit{Equation 2-2}$$

where W is constant power in the adiabatic environment, Δt is the time needed for temperature to increase by infinitesimal value of $\Delta\theta$, M refers to the mass of the specimen, M' is the mass of the specimen holder and C' means the specific heat of the holder. Figure 2-14 presents the specific heat of concrete (Le, 2016).

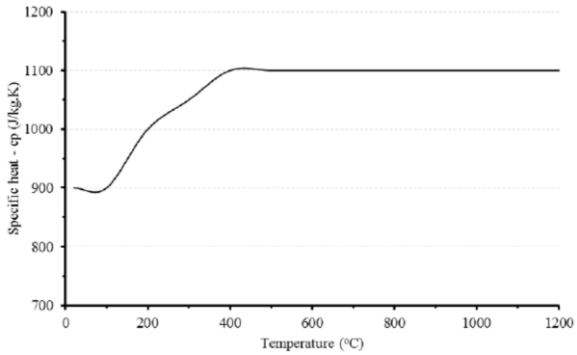

Figure 2-14. Specific heat of concrete (Le, 2016).

c) Thermal conductivity

Thermal conductivity (*k*) indicates the property of HSC to conduct heat. The thermal conductivity of HSC with different aggregate types was tested in the temperature range from 200 to 800 °C and the results are shown in Fig. 2-15 (V. K. R. Kodur & Sultan, 2003).

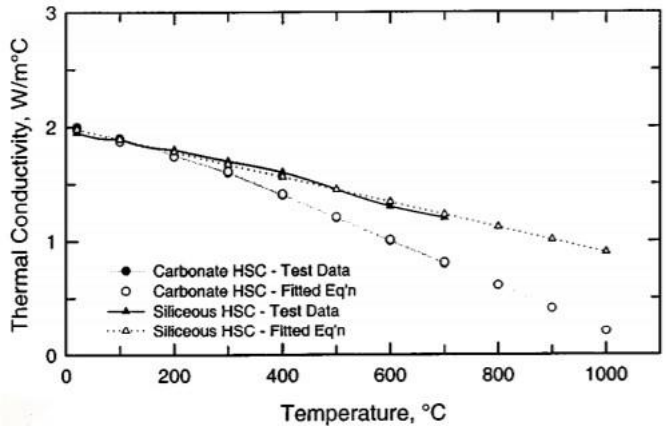

Figure 2-15. Thermal conductivity of HSC with different types of aggregate.

2.3.2. Mechanical properties

The mechanical properties of HSC when exposed to high temperature mainly include compressive strength, elastic modulus, strain at compressive strength and stress-strain curve.

a) Compressive strength

In elevated temperature, HSC has a larger reduction in compressive strength than NSC in high temperature, especially within the temperature range of 100 to 300 °C (Fig. 2-16). In the temperature ranging from 100 to 200°C, the reduction of compressive strength of HSC was 15% to 20% of the original value. One possible reason is that the shrink of the cement and the expansion of aggregate during heating will lead to a loss of bound(Castillo, 1987).

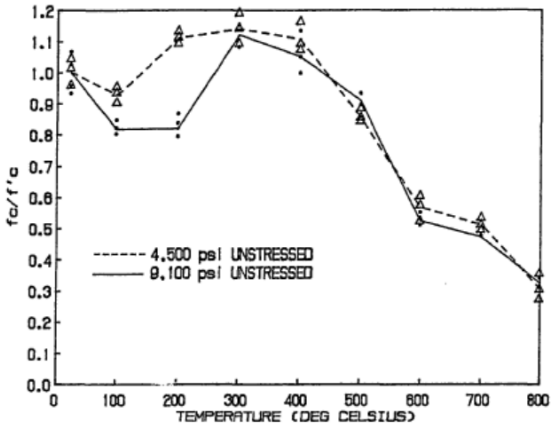

Figure 2-16. Effect of temperature on concrete of different strengths(Castillo, 1987).

b) Elastic modulus

Elastic modulus (E) indicates the ability of HSC to resist being deformed elastically under

loading. It can be expressed as:

$$E = \frac{stress}{strain} \qquad \textit{Equation 2-3}$$

Elastic modulus of HSC with different mixtures all decreased with the rising temperature in both stressed test and unstressed test (Fig. 2-17).

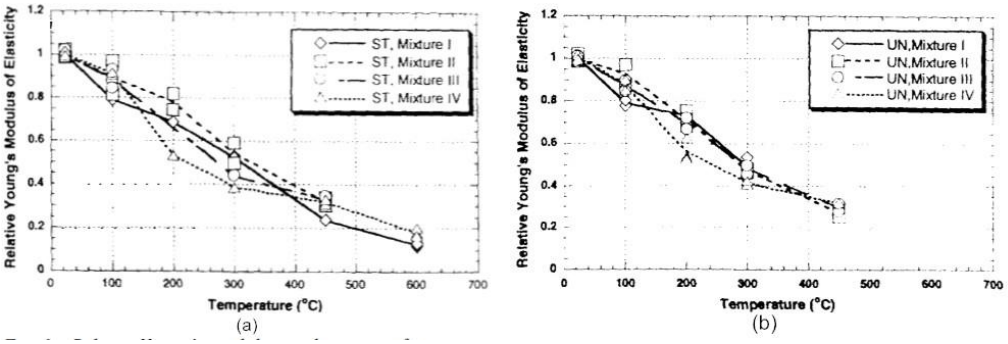

Figure 2-17. Relative Elastic modulus of HSC at elevated temperature under (a) stressed test; b) unstressed test (Phan & Carino, 2002).

c) Strain at compressive strength

The strain of HSC at compressive strength in high temperature can be generated by many factors. Based on EN 1992-1-2 (2004), the total compressive strain is defined as:

$$e = e_s + e_{th} + e_{tr} + e_{creep} \qquad \textit{Equation 4}$$

where e_s is instantaneous stress-dependent strain, e_{th} refers to thermal strain, e_{tr} means the transient state strain and e_{creep} is the creep strain.

d) Stress-strain curve

The stress-strain curves of HSC vary significantly in different temperatures. Due to this, one stress-strain curve can only represent the property of HSC at a constant temperature. The suggested curves for HSC in Australia are shown in Fig. 2-18.

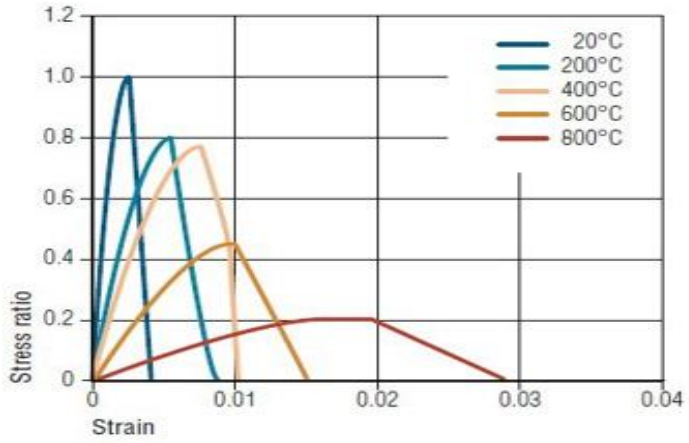

Figure 2-18. Fitted stress-strain curve for HSC (Cement et al., 2010).

Chapter 3. Methods

This chapter will firstly have a detailed illustration of how to apply radiant panels to the fire tests of HSC, in which way a consistent, repeatable and reliable thermal boundary condition can be created. Then it will demonstrate how to apply two deformation measurement methods (actuator and DIC) in the test as well as offer some solutions to the limitations of the measurement methods. Finally, the fire performance tests of HSC will be introduced, including ambient temperature test, unstressed-hot test and stressed-hot test.

All the HSC specimens tested in this experiment are HSC cylinders 200 mm high by 100 mm diameter with f'c = 80 MPa, following Australian Standards (AS 1012.8.1, 2014). After casting for 24 hours and being demolded, all the specimens were placed in water tanks for six days and then kept in a curing room with 23℃ and 50% relative humidity.

3.1 Heat flux calibration

3.1.1. Thermal boundary condition with heat flux

As mentioned in chapter 2, conventioanl furnaces or ovens are not able to offer consistent, repeatable and reliable thermal boundary condition. In order to solve this problem, radiant panels are applied to take the place of funaces. In fire tests with radiant panels, the major form of heat transfer is heat radiation. Based on Fig. 3-1, the incident heat flux imposed on an infinite area (q'_c)can be well calculated by using Equation 3-1.

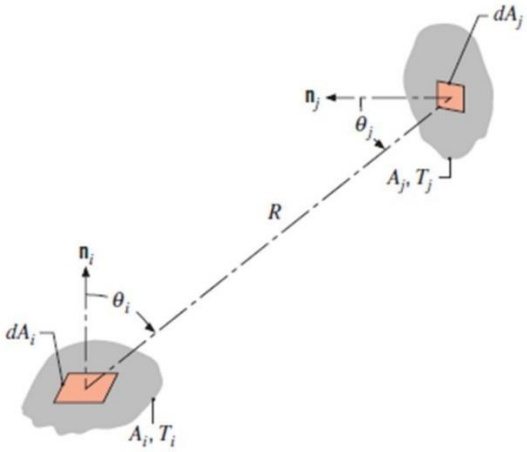

Figure 3-1. View factor associated with radiation exchange(Bergman & Incropera, 2011).

$$q'_c = q' \times \int_{Ap} \frac{cos\theta i cos\theta j}{\pi R^2} dA_p \qquad \text{Equation 3-1}$$

where q' is the maximum radiation heat flux that a radiant panel can offer, A_p refers to the area of a radiant panel, parameters including θi, θj and R can be measured according to the relative position between a radiant panel and the infinite area (Fig. 3-1). Figure 3-2 presents one radiant panel used in the test and the area (A_p) can be easily calculated. Therefore, if the maximum

radiation heat flux of a radiant panel (q') is known, the imposed heat flux on any part of a specimen's surface can be determined. In order to measure the capacity of radiant panels, a water-cooled heat flux sensor is introduced (Fig. 3-3).

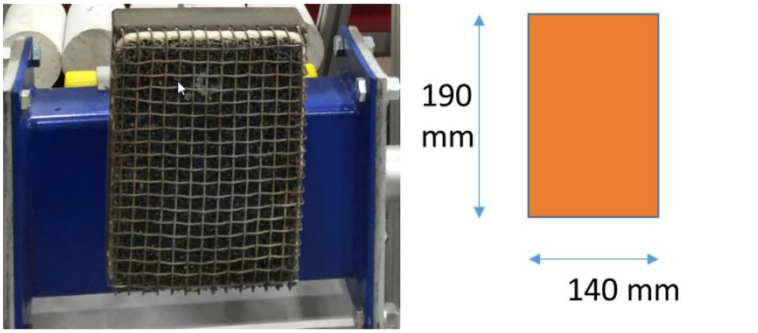

Figure 3-2. A radiant panel and its dimension.

Figure 3-3. Heat flux sensor.

3.1.2. Heat flux calibration test

There are four radiant panels that will be used in the following fire perfomance tests and they are labled as RP1, RP2, RP3, RP4 respectively. In the heat flux calibration text, the capacities of the four radiant panels are measured one by one using heat flux sensor with a distance range 100-300 mm(Fig. 3-4).

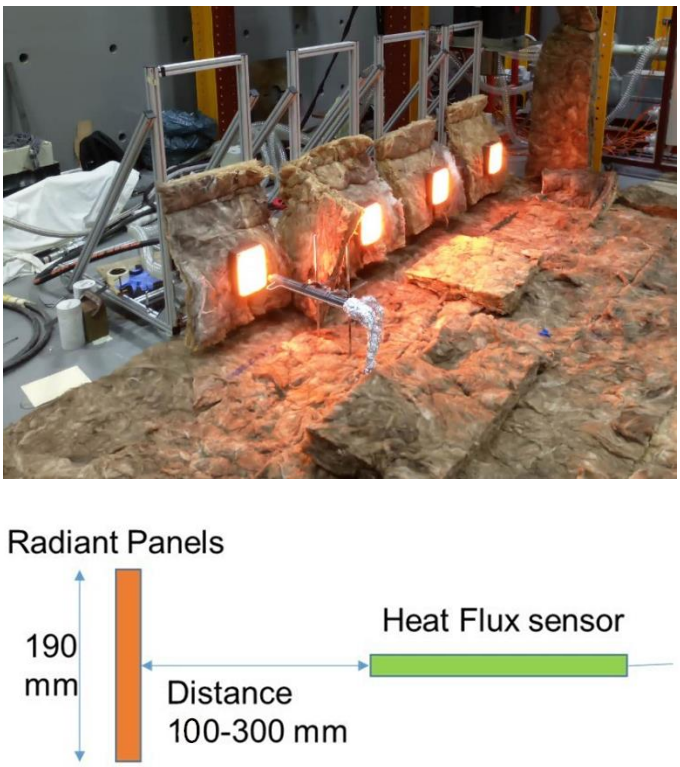

Figure 3-4. Heat flux measurement of RP1(the one on the left).

During the test, the radian panels are moved along a straight line and stopped at six locations (100 mm, 125 mm, 150 mm, 175 mm, 200 mm, 250 mm, 300 mm) for 60 seconds each, so that the heat flux sensor can measure the heat flux at these six distances. The history of distance and heat flux measurement of RP1 to RP4 are shown in Fig. 3-5. It can be seen that with the increase of distance, the incident heat flux imposed on the heat flux sensor is decreasing. After the analysis by using MATLAB, a function curve can be achieved for each of the radiant panels (Fig. 3-5). By extending the curve to the position where the distance is 0 mm, the capacity of the radiant panel can be estimated. In this test, the capacities of RP1 to RP4 are 196.75 kW/m^2, 216.38 kW/m^2, 197.09 kW/m^2 and 205.08 kW/m^2 respectively. As the level of heat flux in the fire performance tests is 20kW/m^2, the distances between the surface of specimens and RP1 to RP4 can be determined through Equation3-1 and the results are 27.05 cm, 30.20 cm, 28.13 cm and 27.48 cm respectively.

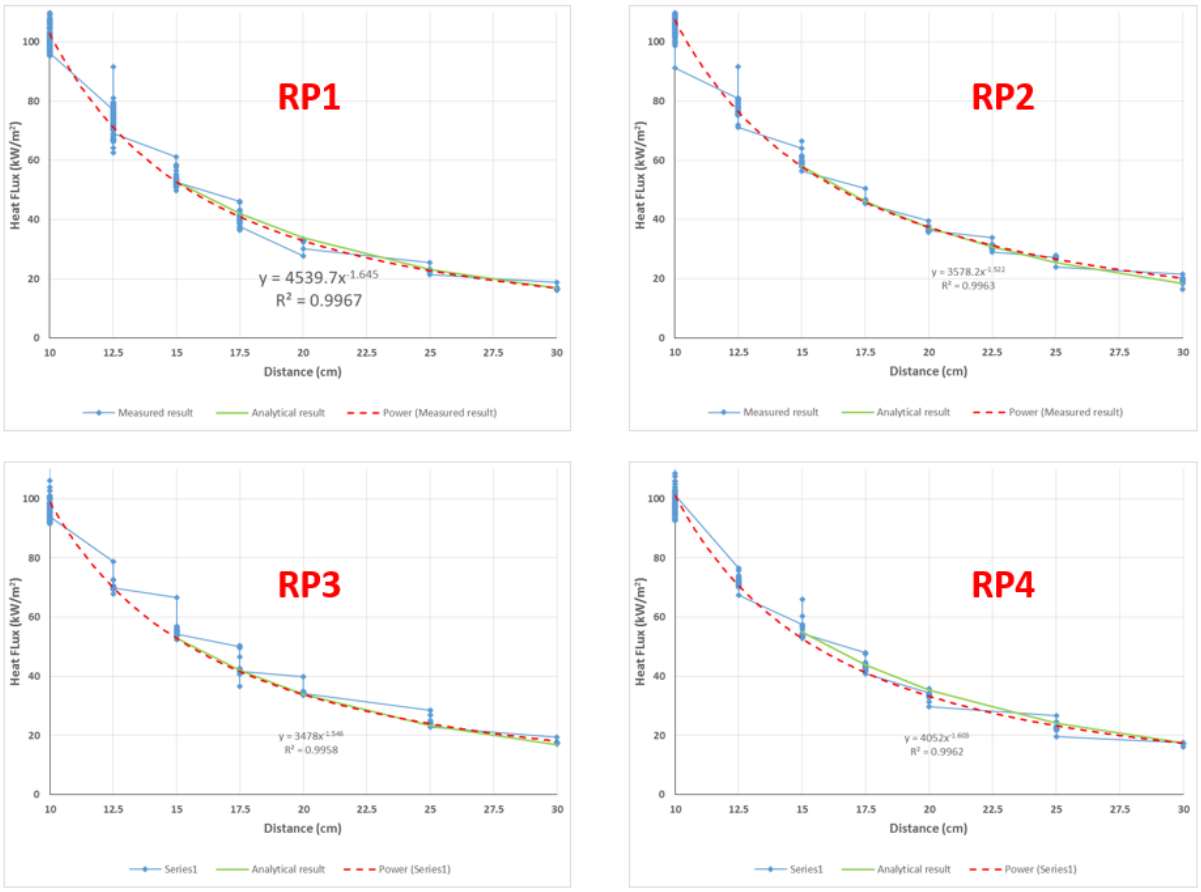

Figure 3-5. Heat flux measurement and analytical results.

According to the work above, the incident heat flux imposed on the middle of HSC cylinder's surface can be well controlled at 20kW/m^2. Therefore, radiant panels can provide a consistent, repeatable and reliable thermal boundary condition.

3.1.3. Test of HSC cylinders with thermocouples

As mentioned in Chapter 2, one stress-strain curve can only represent the property of HSC at a constant temperature. Therefore, the period that it would take for heating the HSC specimens to the target temperature (150℃ in this thesis) with radiant panels should be measured.

Two HSC cylinders with thermocouples were tested to measure the heating period. In the experiment, four radiant panels were located around the HSC cylinder at the distances that have been determined in section 3.1.2 (Fig. 3-6). The average temperature of HSC cylinders during heating can be detected by the thermocouples. Thus, the curve of time and temperature can be recorded. In this test, when the HSC cylinders were heated to 150℃ by radiant panels, it would take 12 minutes and 36 seconds.

Figure 3-6. Test of HSC cylinders with thermocouples.

3.2 Deformation measurement methods

In the fore performance tests of HSC, both actuator and DIC as contact and non-contact methods respectively were applied to measure the deformation of HSC cylinders. The purpose by doing this is to achieve a more reliable measurement results by detecting the same parameter with two different methods. As mentioned in Section 2.2, either actuator or DIC has its own challenges. Therefore, some solutions are figured out to deal with these problems.

3.2.1. Loading frame calibration test

In the compression test, a portal frame equipped with 1 MN actuator (Fig. 3-7) is used to apply load on HSC cylinders. As the displacement measured by actuator contains the deformation of both cylinders and portal frame, the force-dislacement curve of the portal frame should be known before achieveing deformation of HSC cylinders.

Figure 3-7. Loading frame with 1 MN actuator.

A very stiff steel cylinder with the same size of HSC specimens (200 mm high by 100 mm diameter) is utilize to measure the displacements of the loading frame first under different loading conditions. With the increase of force from 0 to 800 kN, the corresponding displacements can be measured by the actuator and recorded by a data logger. The collected displacements are actually the deformation of steel cylinder and loading frame. As the steel cylinder is very stiff, the deformation of it can be equivalent to zero. Thus, we can get the force-displacement curve of the loading frame (Fig. 3-8), which is also called calibration curve in this study for convenience.

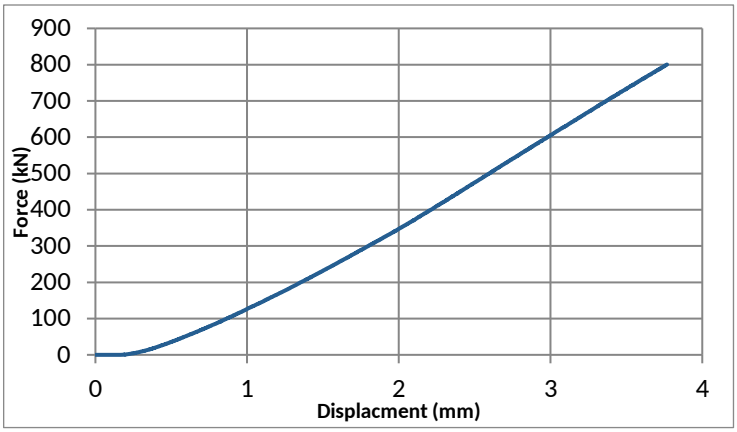

Figure 3-8. Force-displacement curve of the loading frame.

3.2.2. Solutions to the challenges of DIC

There are four main factors that will affect the accurary of DIC in conetional fire resistance testss: windows of funaces, stability of speckle, contrast of image and heat haze. As radiat panels are used instead of conventional funaces in this study, there is no windows between DIC cameras and specimens, which means the influence casued by windows has already been eliminated autamatically. In order to guarantee the stability of the spekle at elevated temperature, ceramic paint which is flame proof (Fig. 3-9) is utilized to paint the spekle patterns. This paint can funtion well at even 1000℃.

Figure 3-9. VHT flame proof paint.

The contrast of image can be influenced bu the quality of spekle patterns and the condition of light. A high-qulity spekle pattern should have a good contrast, clear edges and comsistent images. Two types of spekle patterns are painted on each of the specimens: the white speckles directy on the HSC cylinder and balck speckles with the white blackground colour (Fig. 3-10). The reason of painting two patterns is that balck speckles with the white blackground has a better image constrast, however, it may cause potiential errors of deformation due to its high thickness. Consequencely, one layer white speckles are painted, so that a comparision can be made to see which type of speckle patterns is more suitable in fire resistance tests.

Figure 3-10. Speckle patterns on one HSC cylinder.

As for light condition, the distribution of images can be affected by the light emitted from radiant panels and specimens. As blue bandpass filter on cameras can well limit the wavelength of reflected and emitted light(Novak & Zok, 2011) , a LED with blue light and bandpass filter are utilized to get a good contrast of image (Fig. 3-11).

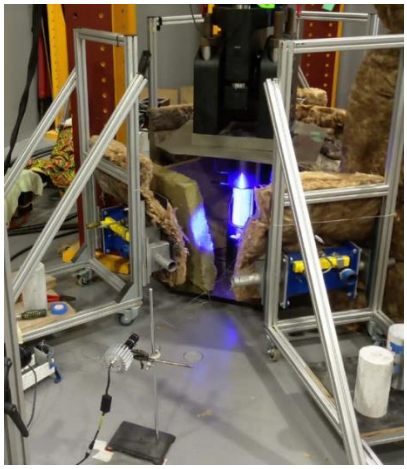

Figure 3-11. Blue LED light and filters on camera.

3.3 Types of tests

There are three types of tests in this study: ambient temperature test, unstressed-hot test and stressed-hot test. In each type of the test, three HSC cylinders were tested one by one. The

test at ambient temperature (about 25 ℃) is to measure the compression strength, stress-strain curve and elastic modulus of specimens. At elevated temperature, as properties of HSC can be changed under different thermal and mechanical loading combination conditions (Anonymous, 2007; V. Kodur & McGrath, 2003; V. K. R. Kodur & Phan, 2007), two types of tests are used in this study: unstressed-hot test and stressed-hot test (Fig. 3-12).

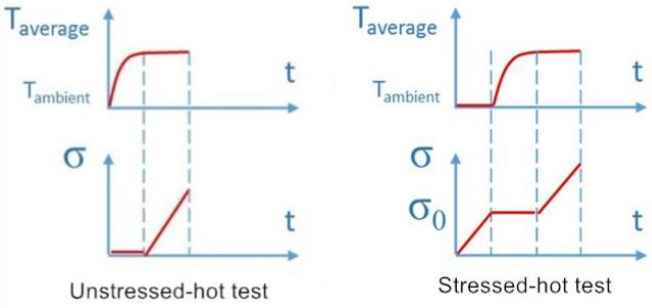

Figure 3-12. Two types of tests at elevated temperature.

In the unstressed-hot test, the HSC cylinders were heated for 12 minutes and 36 seconds to reach the target temperature (150℃) without loading and then loaded to failure at 150℃. In the stressed test, a pre-compression load which is selected as 20% of ultimate strength of specimens at ambient temperature was applied on the HSC cylinders first. Then, the HSC cylinders were heated for 12 minutes and 36 seconds to 150℃ with the load, after which they were loaded to failure at 150℃.

Four radiant panels located on the trolleys were placed around the cylinder and utilized for heating, controlling the incident heat flux imposed on the middle of HSC cylinder's surface at 20kW/m^2 (Fig. 3-13).

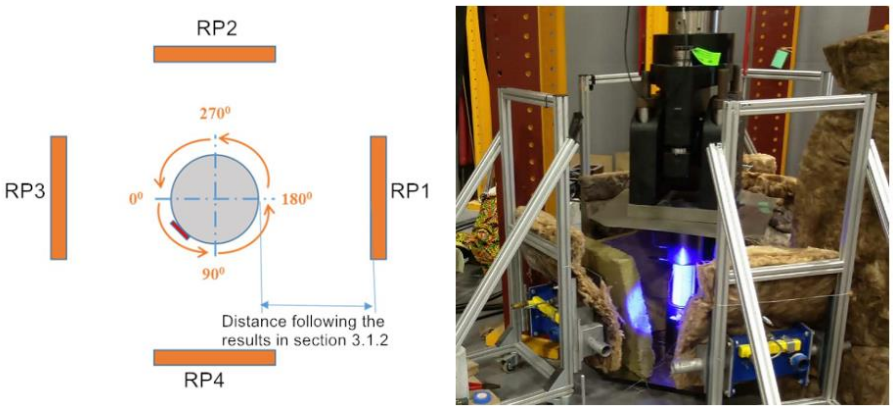

Figure 3-13. Arrangement of radiant panels.

In ambient temperature test, the deformations of HSC cylinders were measured by strain gauges which were attached on the surface of cylinder, actuator and DIC. While in unstressed-hot test and stressed-hot test, the deformations were measured by actuator and DIC.

Chapter 4. Results and Discussion

In this chapter, the results of the tests are presented. Comparisons between the properties of HSC in high temperature and in ambient temperature will be made, including compressive strength, displacement, stress-strain curve and elastic modulus of HSC.

4.1 Results of ambient temperature test

Figure 4-1 shows the force-displacement curves of the three specimens at ambient temperature. The curves named 'DIC.BoW' and 'DIC.W' are the results measured by DIC with black and white speckle pattern and white speckle pattern respectively, while the curve named 'Calculated' is the result measured by actuator. One thing need to pay attention to is that the 'Calculated' curve is achieved by decreasing the direct results of actuator by calibration curve.

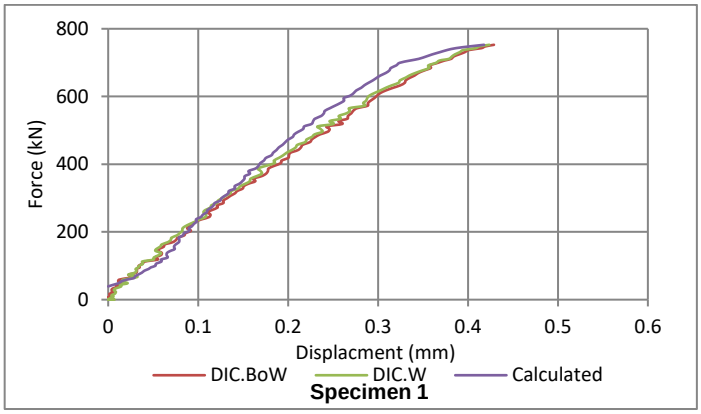

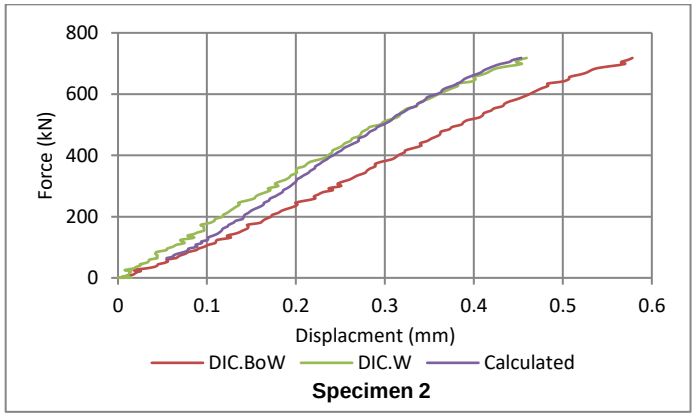

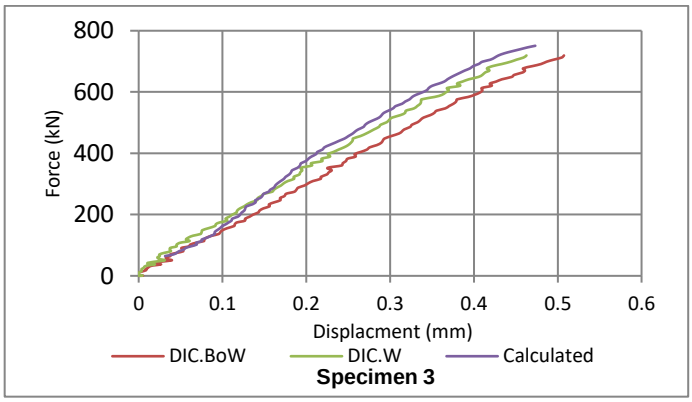

Figure 4-1. Force-displacement curves of HSC cylinders at ambient temperature.

It can be seen that the maximum axial forces that the three HSC cylinders can bear are 753kN, 718 kN and 751 kN respectively (Fig. 4-1). The compression strengths are 95.8 MPa, 91.4 MPa and 95.6 MPa, and the average is 94.3 MPa.

The stress-strain curves of the three specimens at ambient temperature are presented in Fig. 4-2. The curves named ‘SG1’ and ‘SG2’ are measured by the two strain gauges attached on the cylinders.

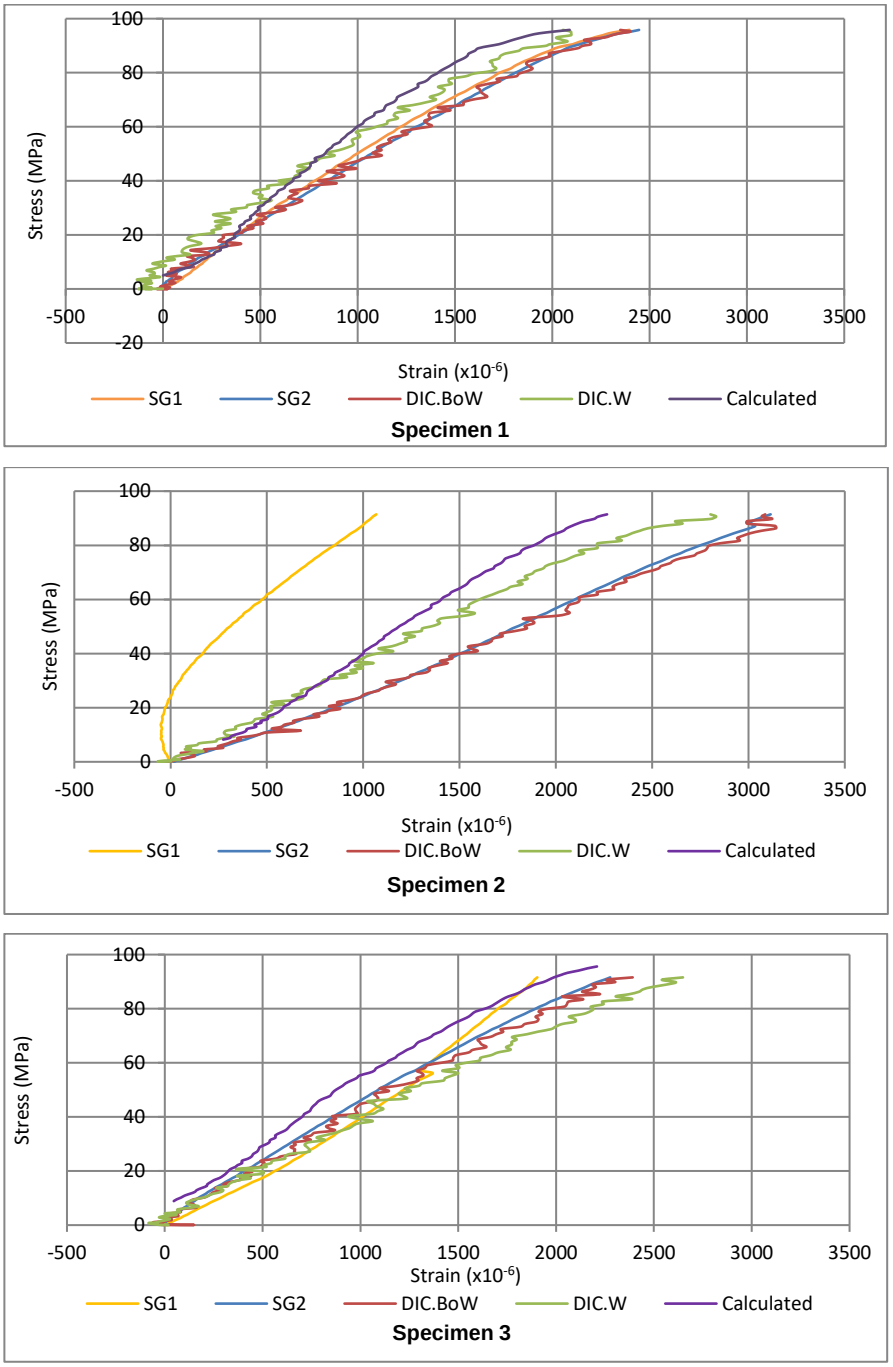

Figure 4-2. Stress-strain curves of HSC cylinders at ambient temperature.

It can be seen the stress-strain curves of the three specimens measured by three different methods fit well. This means that strain gauges, actuator and DIC can measure deformation

reliably at ambient temperature. However, in specimen 2, the curve measured by SG1 varies significantly with others. The possible reason can be that SG1 is damaged or the connection between the strain gauge and the specimen becomes loose during the test.

4.2 Results of unstressed-hot test

Figure 4-3 shows the force-displacement curves of the HSC cylinders in unstressed-hot test at 150℃.

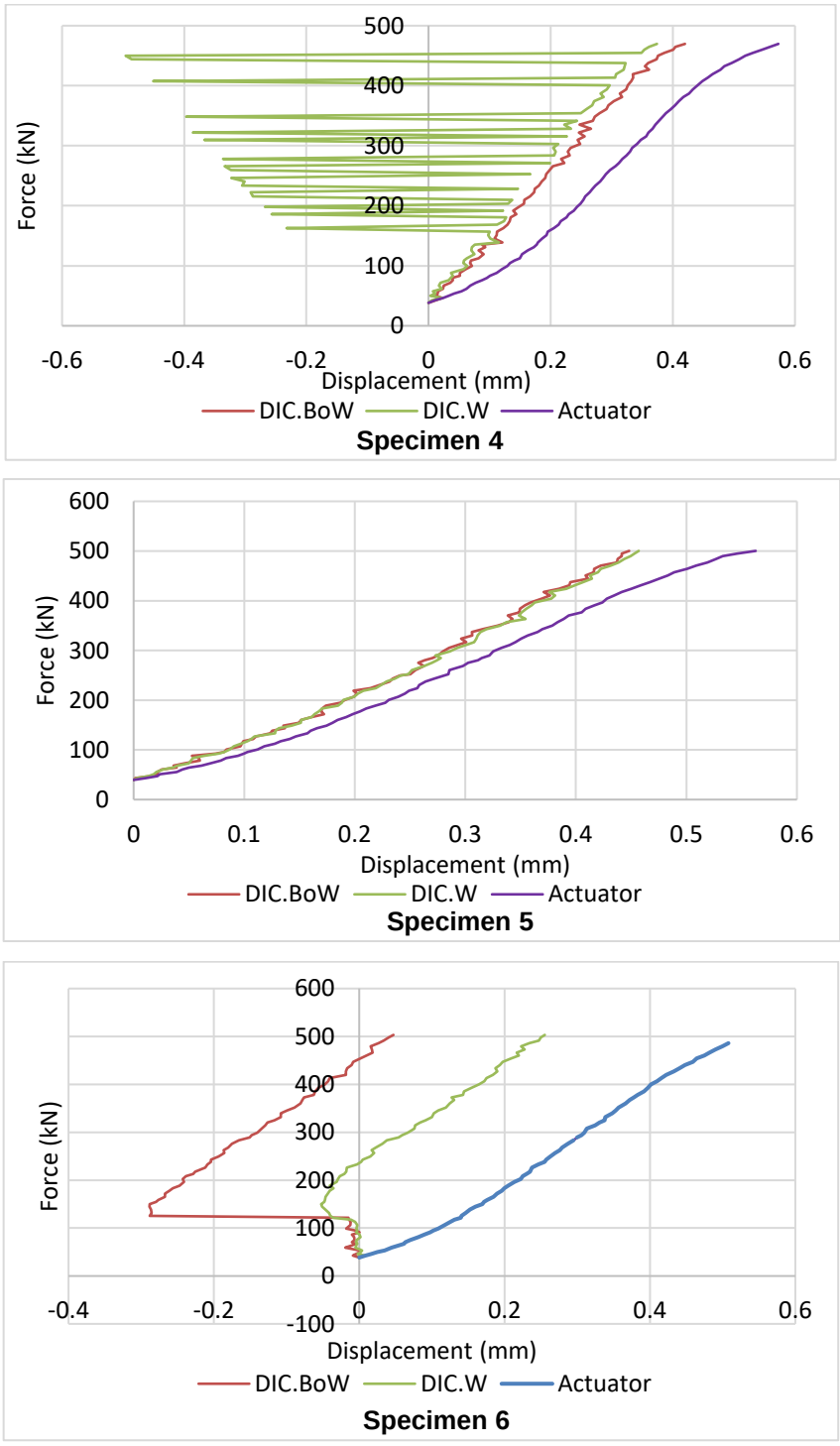

Figure 4-3. Force-displacement curves of HSC cylinders in unstressed-hot test at 150 ℃.

The maximum axial forces that the three HSC cylinders can sustain are 470 kN, 500 kN and 503 kN respectively (Fig. 4-3). The compression strengths are 59.8 MPa, 63.7 MPa and 64.1 MPa, and the average is 62.5 MPa. In specimen5, the curves measured by DIC and actuator have a high-level fit. However, the curve of specimen 4 measured by DIC with white speckle patterns has great fluctuations, which shows a failure in measurement. The possible reason might be the instability of white patterns after heating. In specimen 6, the slopes of the three curves are similar, but have significant deviations at the beginning of compression.

The stress-strain curves of the three specimens in unstressed-hot test at 150℃ are presented in Fig. 4-4. The results of DIC.W in specimen 4 is erased due to the fluctuations. In specimen 4 and specimen 5, curves measured by DIC and actuator have a good match and the elastic modulus (the slope of the curve) of these two HSC cylinders are similar. However, the curves of specimen 6 are not satisfactory. The three curves have significant differences, including the slope and the value. This may be because that the quality of specimen 6 is not as good as other specimens, leading to a uniform deformation.

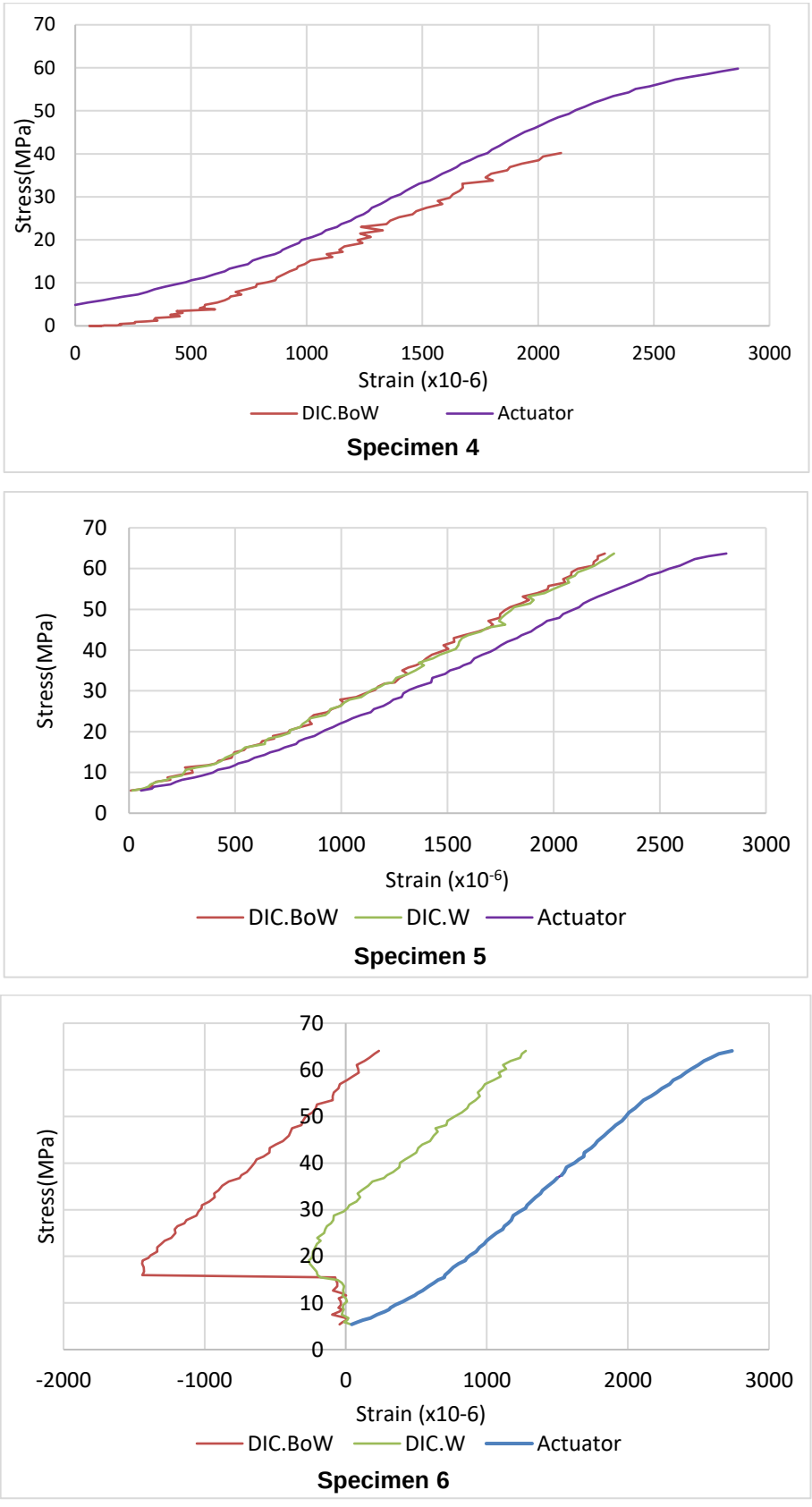

Figure 4-4. Stress-strain curves of HSC cylinders in unstressed-hot test at 150 ℃.

4.3 Results of stressed-hot test

Figure 4-5 presents the force-displacement curves of the HSC cylinders in stressed-hot test at 150℃.

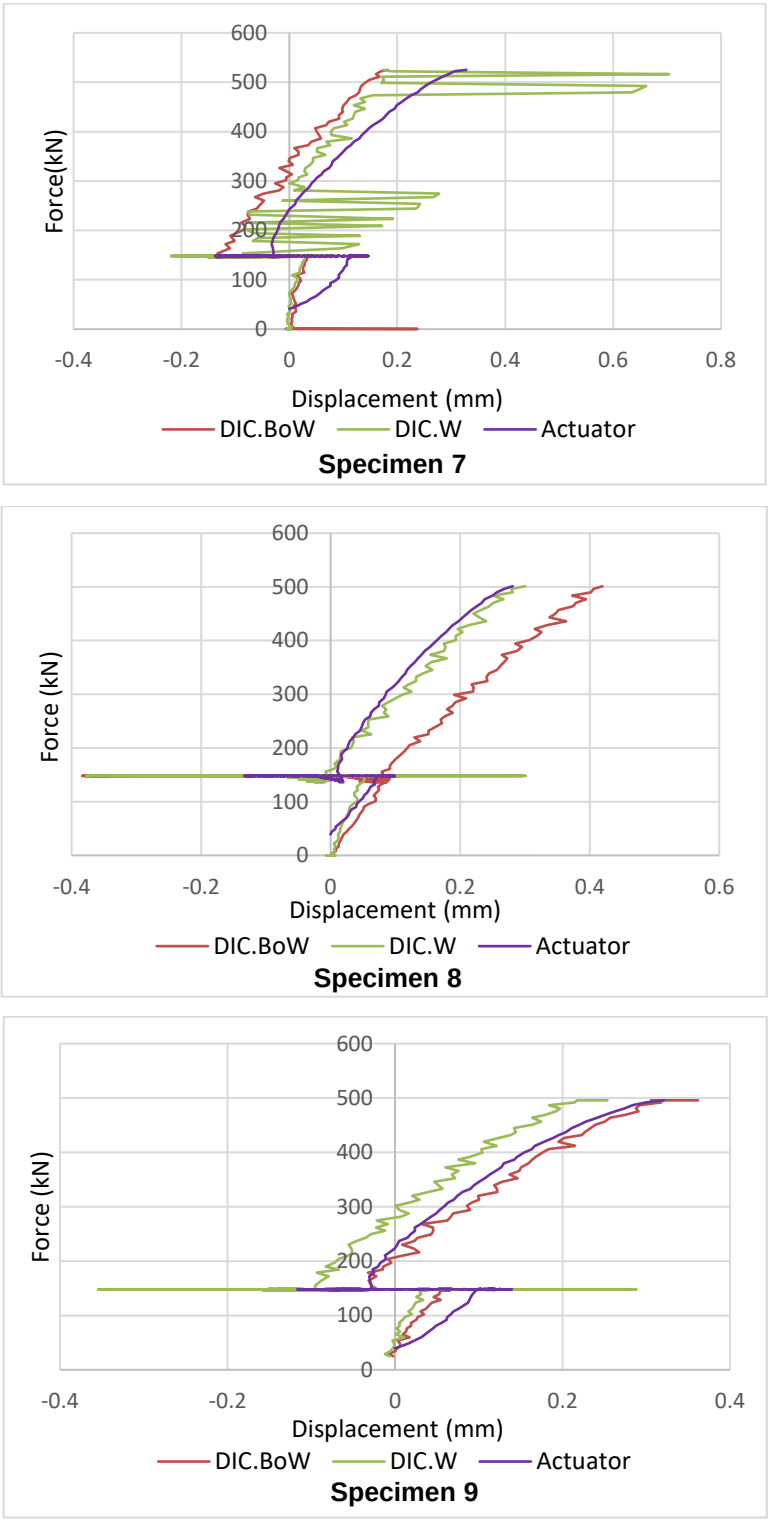

Figure 4-5. Force-displacement curves of HSC cylinders in stressed-hot test at 150 ℃.

The maximum axial forces that the three HSC cylinders can hold are 511 kN, 501 kN and 496 kN respectively (Fig. 4-5). The compression strengths are 65.1 MPa, 63.8 MPa and 63.1

MPa, and the average is 64 MPa. In specimen5, the curves measured by DIC and actuator have a high-level fit. However, the curve of specimen 7 measured by DIC with white speckle patterns has significant fluctuations, which has a similar situation in specimen 4. Meanwhile, DIC with 'black on white' speckle patterns performed well in all six heated cylinders. Therefore, compared with white speckle pattern, the 'black on white' speckle pattern is more stable and endurable at elevated temperature.

The stress-strain curves of the three specimens in stressed-hot test at 150℃ are presented in Fig. 4-6. The results of DIC.W in specimen 7 is erased according to the unreliable measurement. The curves of the three specimens measured by DIC and actuator match well, which indicating that both DIC and actuator are reliable measurement methods in fire resistance tests.

All the three specimens have displacements during heating with pre-compression load (Fig. 4-6). The strain during this process is named load induced thermal strain (LITS), which generates when concrete is heated while under compressive stress condition (Torelli, Gillie, Mandal, & Tran, 2017).

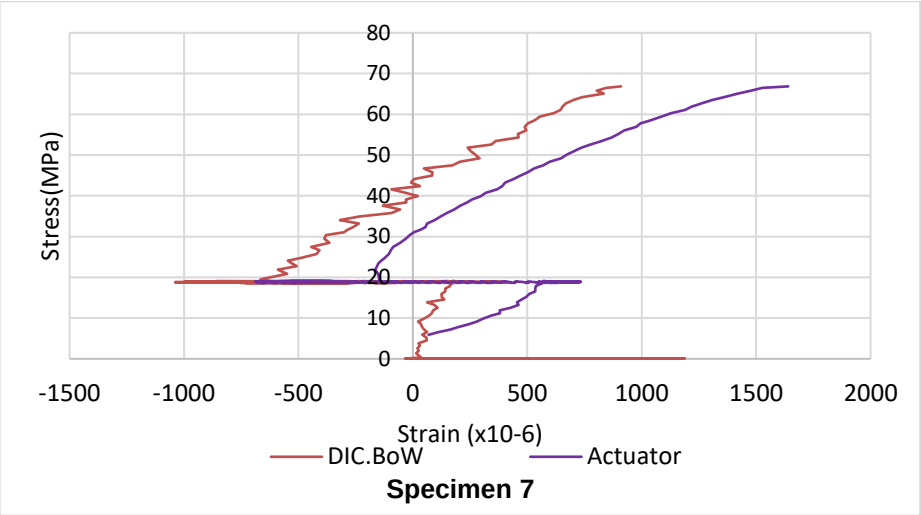

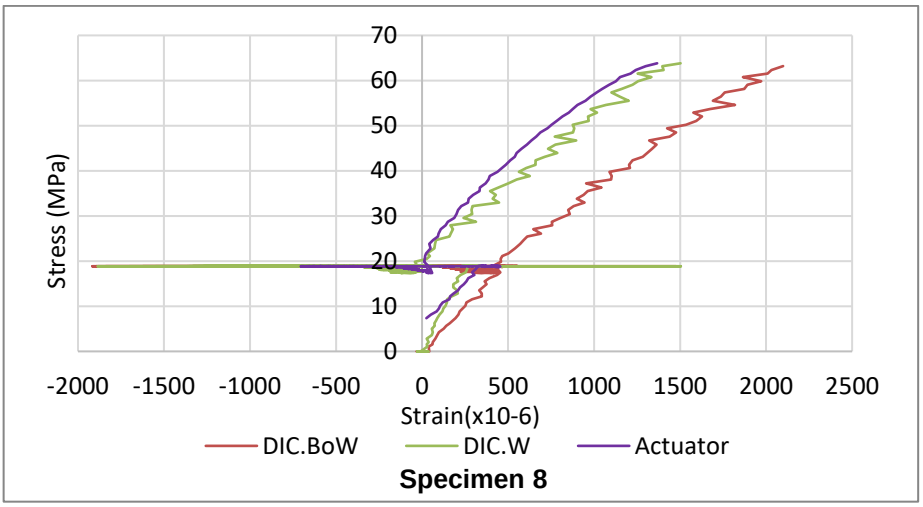

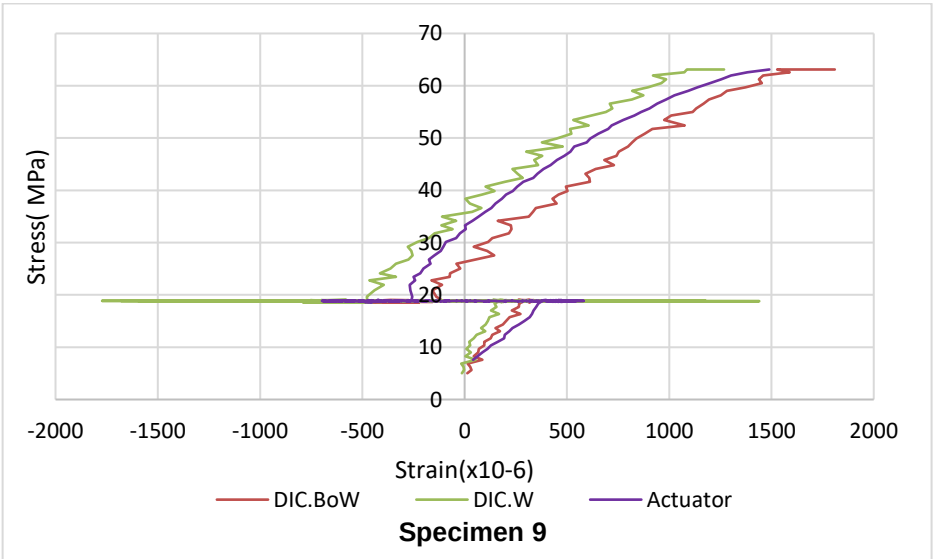

Figure 4-6. . Stress-strain curves of HSC cylinders in stressed-hot test at 150 ℃.

4.4 Comparisons among the tests

4.4.1. Compressive strength

Figure 4-7 shows the average compression strengths of the HSC cylinders in each type of

the tests. It can be seen that the compression strength of HSC will decrease with the increase of the temperature. In comparison with the compression strength at ambient temperature, the reduction of compression strengths of HSC in the unstressed-hot test and stressed-hot test at 150℃ can be up to 33.7% and 36% respectively. What is more, the combination conditions of thermal and mechanical loading have a limited impact on the degradation of HSC compression strength.

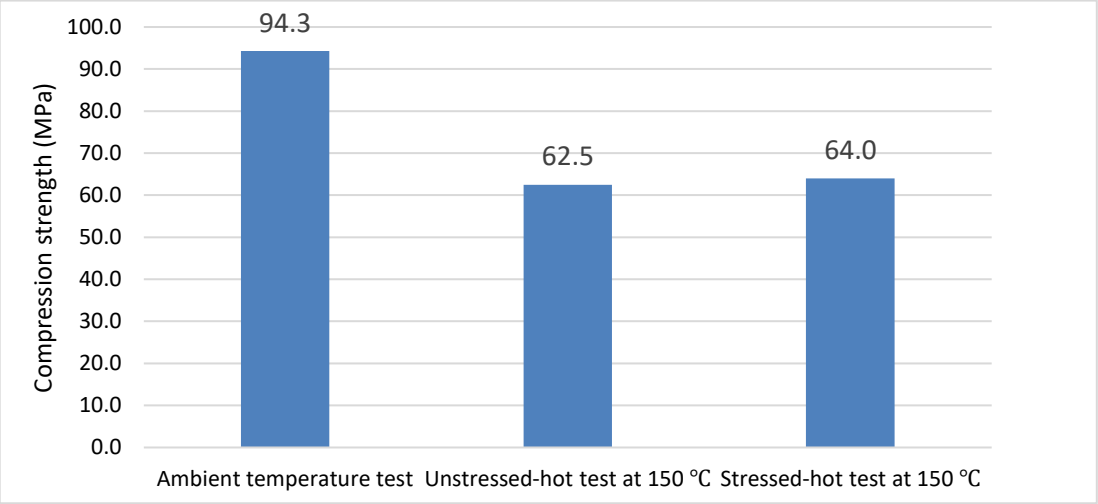

Figure 4-7. Compression strengths of specimens in the different tests

4.4.2. Elastic modulus

According to the stress-strain curves, the elastic modulus of HSC in the ambient temperature test, unstressed-hot test at 150℃ and stressed-hot test at 150℃ can be achieved and the results are 44750 MPa, 21640 MPa and 30100 MPa respectively. Therefore, the elastic modulus of HSC will decrease as a consequence of the rising temperature. Besides, the elastic modulus reduction caused by heating without loading is larger than heating with pre-compression.

Chapter 5. Conclusions and Suggestions

5.1 Conclusions

The major contributions of this thesis can be concluded as follows:

i. A reliable and consistent thermal boundary condition has been set up by using radiant panels to examine the performance of HSC at elevated temperature.

ii. Two different deformation measurement methods, which are actuator and DIC, are applied in the test to measure the deformation of HSC cylinders. A series of solutions has been figured out to deal with the challenges of actuator and DIC, and the results are satisfactory.

iii. Mechanical properties of HSC at ambient temperature and elevated temperature have been examined, including compressive strength, stress-strain curves and elastic modulus.

5.2 Suggestions for future work

There still exist some limitations of this thesis. The suggestions for future work are presented as follows:

i. In the radiant panel system, the main parameter of fire is suggested as incident heat flux. In this thesis, all the HSC cylinders were tested with the incident heat flux level of 20kW/m^2. In order to achieve a more reliable result, more tests with different levels of incident heat flux should be done.

ii. Due to the limitation of time, the properties of HSC achieved in the thesis are at 150℃. More specimens should be tested at different temperatures, so that the properties of HSC can be better examined.

iii. Although radiant panel system can provide a consistent and reliable thermal boundary condition, there still exists heat loss caused by heat convection during the test. In this test, thermal isolations were used to eliminate the heat loss. However, it cannot totally prevent the loss of heat. Thus, more investigation can be done on this part to rid of the influences.

References

Anagnostopoulos, N., Sideris, K., & Georgiadis, A. (2009). Mechanical characteristics of self-compacting concretes with different filler materials, exposed to elevated temperatures. *Materials and Structures, 42*(10), 1393-1405. doi:10.1617/s11527-008-9459-6

Anonymous. (2007). Recommendation of RILEM TC 200-HTC: mechanical concrete properties at high temperatures—modelling and applications. *Materials and Structures, 40*(9), 855-864. doi:10.1617/s11527-007-9286-1

AS 1012.8.1. (2014). Methods of Testing Concrete. Method 8.1: Method for making and curing concrete - Compression and indirect tensile test specimens. Australia: Standards Australia.

Bergman, T. L., & Incropera, F. P. (2011). *Fundamentals of heat and mass transfer* (7th ed. / Theodore L. Bergman ... [et al.].. ed.). Hoboken, NJ: Hoboken, NJ : Wiley.

Castillo, C. (1987). Effect of transient high temperature on high-strength concrete. In A. J. Durrani (Ed.): ProQuest Dissertations Publishing.

Cement, C., amp, & Aggregates, A. (2010). *Fire safety of concrete buildings / Cement Concrete & Aggregates Australia*. Australia: Australia : Cement Concrete & Aggregates Australia.

Chan, S. Y. N., Peng, G. F., & Chan, J. K. W. (1996). Comparison between high strength concrete and normal strength concrete subjected to high temperature. *Materials and Structures, 29*(194), 616-619. doi:Doi 10.1007/Bf02485969

EN 1992-1-2. (2004). 1-2: 2004 Eurocode 2: Design of concrete structures-Part 1-2: General rules- Structural fire design. European Standards, London.

Fsh. (2008). *BS 9999:2008 - Code of practice for fire safety in the design, management and use of buildings*.

Giri, P., Kharkovsky, S., & Samali, B. (2017). Inspection of Metal and Concrete Specimens Using Imaging System with Laser Displacement Sensor†. *Electronics, 6*(2), 36. doi:10.3390/electronics6020036

Hoffmann, K. (1989). *An introduction to measurements using strain gages : with 172 figures and tables / Karl Hoffmann*. Darmstadt: Darmstadt : Hottinger Baldwin Messtechnik GmbH.

Hu, Z., Xie, H., Lu, J., Hua, T., & Zhu, J. (2010). Study of the performance of different subpixel image correlation methods in 3D digital image correlation.(Author abstract)(Report). *Applied Optics, 49*(21), 4044. doi:10.1364/AO.49.004044

Ingberg, S. H., Griffin, H. K., Robinson, W. C., & Wilson, R. E. (1921). Fire tests of building columns. *Journal of the Franklin Institute, 191*(6), 823-827. doi:10.1016/S0016-0032(21)90681-1

Jacob, B. (1870). Fire-Proof Construction. Scientific American, 23(16), 245-245. Retrieved from http://www.jstor.org/stable/26032068.

Kakae, N., Miyamoto, K., Momma, T., Sawada, S., Kumagai, H., Ohga, Y., . . . Abiru, T. (2017). Physical and Thermal Properties of Concrete Subjected to High Temperature. *J. Adv. Concr. Technol., 15*(6), 190-212. doi:10.3151/jact.15.190

Kayser, P., Godefroy, J. C., & Leca, L. (1993). High-temperature thin-film strain gauges. *Sensors & Actuators: A. Physical, 37*(1), 328-332. doi:10.1016/0924-4247(93)80055-L

Kendall, J. (1912). Fire Prevention and Fire Protection as applied to Building Construction (Vol. 5, pp. 471-471). London: Builder, Society of Architects.

Kesavan, S. and Reddy, N. 2006. Linear Variable Differential Transformers. Encyclopedia of Medical Devices and Instrumentation.

Khoury, G., Grainger, B., & Sullivan, P. (1985). Transient thermal strain of concrete: literature review, conditions within specimen and behaviour of individual constituents.

Magazine of Concrete Research, 37, 131-144.
Kodur, V., & McGrath, R. (2003). Fire Endurance of High Strength Concrete Columns. *Fire Technology, 39*(1), 73-87. doi:10.1023/A:1021731327822
Kodur, V. K. R., & Phan, L. (2007). Critical factors governing the fire performance of high strength concrete systems. *Fire Safety Journal, 42*(6), 482-488. doi:10.1016/j.firesaf.2006.10.006
Kodur, V. K. R., & Sultan, M. A. (2003). Effect of Temperature on Thermal Properties of High-Strength Concrete. *Journal of Materials in Civil Engineering, 15*(2), 101-107. doi:10.1061/(ASCE)0899-1561(2003)15:2(101)
Le, Q. X. (2016). A study of temperature gradient effects on mechanical properties of concrete at elevated temperatures (MPhil), The University of Queensland
Malladi, S. (2015). Fiber optic sensors and digital signal processing in displacement measurements. In R. Guo, A. Bhalla, & Y. Joo (Eds.): ProQuest Dissertations Publishing.
Maluk, C., Bisby, L., Terrasi, G., Krajcovic, M., & Torero, J. L. (2012). Novel fire testing methodology: Why, how and what now?
Maluk Zedan, C. H. (2014). Development and application of a novel test method for studying the fire behaviour of CFRP prestressed concrete structural elements. In L. Bisby & T. Stratford (Eds.): University of Edinburgh.
McAllister, T., Luecke, W., Iadicola, M., & Bundy, M. (2012). Measurement of Temperature, Displacement, and Strain in Structural Components Subject to Fire Effects: Concepts and Candidate Approaches, National Institute of Standards and Technology,US.
Micro-Epsilon. (2008). MICRO-EPSILON Instruction Manual - OptoNCDT 1302. In Micro-Epsilon (Ed.), Orenburg, Germany.
Miller R.P. and Stewart P.M. (1902). Making Buildings Safe: Fireproof Materials and Methods of Construction. Proceeding of the National Association of Cement Users, 185-197.
Mostafaei, H. (2013). Hybrid fire testing for assessing performance of structures in fire—Application. *Fire Safety Journal, 56*, 30-38. doi:10.1016/j.firesaf.2012.12.003
NFPA (1914). Report of Committee on Fire-Resistive Construction, Proceedings of the 18th National Fire Protection Association Annual Meeting, Boston, US, 216-227.
NFPA (1918). Report of Committee on Fire-Resistive Construction, Proceedings of the 22th National Fire Protection Association Annual Meeting, Boston, US, 170-221.
Novak, M. D., & Zok, F. W. (2011). High-temperature materials testing with full-field strain measurement: Experimental design and practice. *Review of Scientific Instruments, 82*(11). doi:10.1063/1.3657835
Phan, L. T., & Carino, N. J. (2002). Effects of test conditions and mixture proportions on behavior of high-strength concrete exposed to high temperatures. *ACI Materials Journal, 99*(1), 54-66. doi:10.14359/11317
Sachs (1903). Suggested Standard of Fire Resistance. Report of Proceedings of the International Fire Prevention Congress, London, UK, 243-248.
Sounthararajah, A., Wong, L., Nguyen, N., Bui, H. H., & Kodikara, J. (2017). Evaluation of flexural behaviour of cemented pavement material beams using distributed fibre optic sensors. *Construction and Building Materials, 156*, 965-975. doi:10.1016/j.conbuildmat.2017.09.027
Sultan, M. A. (2010). Comparisons of Temperature and Heat Flux in Furnaces Controlled by Different Types of Temperature Sensors. *Journal of ASTM International, 7*(1), 1-13. doi:10.1520/JAI102334
Torelli, G., Gillie, M., Mandal, P., & Tran, V.-X. (2017). A multiaxial load-induced thermal strain constitutive model for concrete. *International Journal of Solids and Structures, 108*, 115-125. doi:10.1016/j.ijsolstr.2016.11.017

Torero, J. (2014). Assessing the performance of concrete structures in fires. Concrete in Australia- Special Issue on" Concrete Performance in Fire, 40(3), 44-49.
Voigt, A. (2010). Evaluation of methods for measuring concrete modulus of elasticity. In D. Mukai, C. Dolan, & D. Walrath (Eds.): ProQuest Dissertations Publishing.
Yuan, S. (2014). Digital image correlation and edge detection: Applications in materials testing. In J. Giancaspro, C. Hays, A. Nanni, & Q. Yang (Eds.): ProQuest Dissertations Publishing.
Yabuki Y., Harada K., and Terai T. (1995). Heat transfer in fire resistance test furnace with particular references to gas radiation. Proceedings of the 2nd Asia - Oceanian conference on Fire Science and Technology, 262-273.